ACS SENSORS

pubs.acs.org/acssensors

Article

# Rapid Assessment of Meat Freshness by the Differential Sensing of Organic Sulfides Emitted during Spoilage

Xinting Yu, Yanjun Gong, Hongwei Ji, Chuanqin Cheng, Chunxiao Lv,* Yifan Zhang, Ling Zang, Jincai Zhao, and Yanke Che*

Cite This: *ACS Sens.* 2022, 7, 1395−1402

Read Online

ACCESS | Metrics & More | Article Recommendations | Supporting Information

**ABSTRACT:** In this work, we report the fabrication of a two-member fluorescence sensor array that enables the assessment of three stages (fresh, slightly spoiled, and moderately or severely spoiled) of meat spoilage. The first member of the array, which has strong chalcogen bonding and sulfur−$\pi$ interactions with organic sulfides, exhibits very high sensitivity, while the second member of the array, which has weak chalcogen bonding and sulfur−$\pi$ interactions with organic sulfides, exhibits lower sensitivity. On the basis of the combined fluorescence responses of the two members, three stages of meat spoilage, including fresh, slightly spoiled, and moderately or severely spoiled, can be monitored. Notably, using the volatiles collected from 5 g of meat products over a short period of time (1 min), this two-member sensor array achieves sensitive responses to the organic sulfides emitted from the meats. The capacity of this method to rapidly assess meat freshness facilitates its practical application, as illustrated by the monitoring of the freshness of chicken and pork products in the real world.

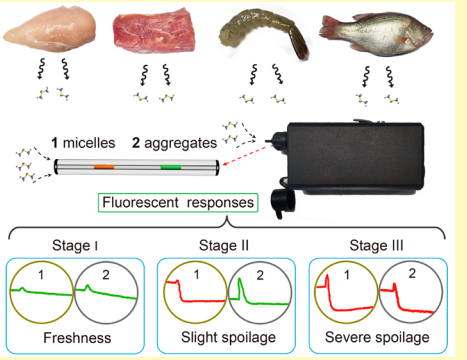


**KEYWORDS:** *chalcogen bonding, sulfur−$\pi$ interactions, differential sensing, organic sulfides, meat freshness*



Compared with solution-based detection techniques, the volatile-based detection of specific volatile organic compounds (VOCs), e.g., amines, emitted from meat products represents a convenient sensing method for monitoring meat freshness.[1−12] However, for nearly all reported detection technologies, including electronic noses and optical sensors,[1,2,5−12] the absolute concentrations of amines and other VOCs need to be accumulated to trigger sensor responses for the assessment of meat freshness. These collection and concentration processes generally require long periods of time (hours or even days), which is far from satisfactory for real-world applications. Furthermore, the accurate concentration of specific VOCs (e.g., amines), which is key for conducting freshness assessments, is difficult to achieve at the ppb levels in complex environments. Given these disadvantages of the current volatile-based detection technologies that greatly limit their practical applications for monitoring meat freshness, there remains an urgent need to develop reliable technologies for the rapid and precise assessment of meat freshness.

As a detection technology that is fast, sensitive, and humidity-tolerant,[1,2,8−23] fluorescence sensing has been widely investigated for monitoring meat freshness, particularly via the detection of accumulated volatile amines emitted from spoiled meats.[1,2,8−12] However, amines form strong hydrogen bonds with many other components (e.g., amino acids and water) or exist in their protonated forms at the buffered pH of biological matrices; therefore, they are not easily released from meat. Therefore, collecting a sufficient concentration of volatilized amines within a short period of time is challenging, particularly during the early stages of meat spoilage. To address this problem, the fast and sensitive detection of specific components that are easily collected in the gas phase during spoilage is needed. Given that organic sulfides, e.g., dimethyl sulfide, have no strong interactions with other components, they can be released easily and thus may not require a long-term accumulation process and act as a suitable marker for the rapid assessment of meat freshness in the real world. Of note, hydrogen sulfide is mainly released during the advanced stages of spoilage[24,25] and therefore is not suitable for the precise monitoring of meat freshness. However, the fluorescence detection of trace levels of organic sulfides in gaseous mixtures obtained from meat products has not been explored for the assessment of meat freshness.

In this work, we developed a two-member sensor array composed of two donor−acceptor (D-A) fluorophores **1**−**2** with differential sensitivities to organic sulfides emitted from meat products. Specifically, fluorophore **1** shows strong

**Received:** January 11, 2022
**Accepted:** April 4, 2022
**Published:** April 14, 2022




https://doi.org/10.1021/acssensors.2c00079
*ACS Sens.* 2022, 7, 1395−1402

chalcogen bonding and sulfur−$\pi$ interactions with organic sulfides, which trigger a sensitive fluorescence quenching response, thereby enabling it to signal a transition in meat from fresh (Stage I) to slightly spoiled (Stage II). In contrast, fluorophore **2** shows weak chalcogen bonding and sulfur−$\pi$ interactions with organic sulfides, which triggers weak quenching responses. However, it can assist in the assessment of the extent of spoilage, i.e., from slight to moderate to severely spoiled. Notably, this two-member sensor array achieves sensitive responses to the organic sulfides present in gaseous mixtures collected from meat products over a short period of time (1 min); that is, various other VOCs, including amines, cannot mask the responses of the sensor array to the organic sulfides. The rapid assessment of meat freshness paves the way for applying fluorescence sensors for monitoring meat freshness in the real world.

## EXPERIMENTAL SECTION

**Synthesis and Self-Assembly of Fluorophores 1 and 2.** Scheme 1 shows the synthesis route for fluorophore **1**. Fluorophore **2**

**Scheme 1. Synthesis Route for Fluorophore 1**

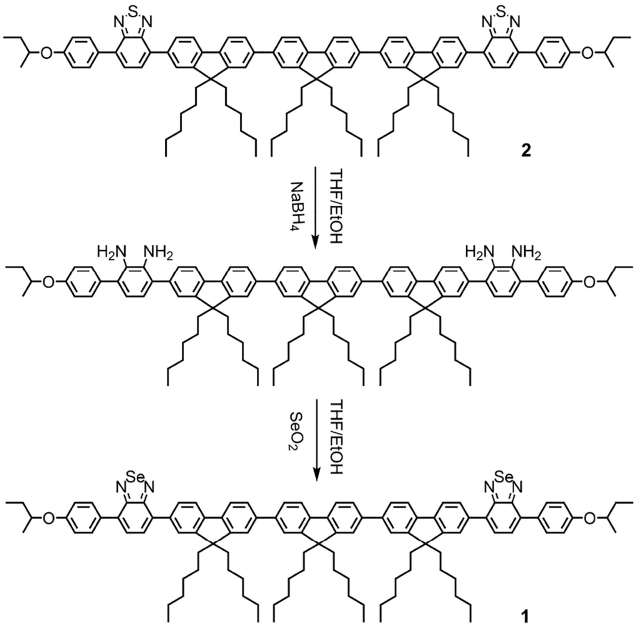


was synthesized following a previously reported method.[13] The detailed synthesis and characterization of fluorophore **1** are described in the Supporting Information. The micelles from fluorophore **1** (**1** micelles) and the aggregates from fluorophore **2** (**2** aggregates) were self-assembled by injecting 0.1 mL of a chloroform solution of fluorophores **1** and **2** (6 mg/mL) into a vial containing 1 mL of methanol, respectively, and aging for 1 d at room temperature. The resulting assemblies suspended in the solutions were then cast onto various substrates and into a quartz tube.

**Structure and Optical Characterization.** Scanning electron microscopy (SEM) images were obtained on a Hitachi SU8010 field-emission microscope. The SEM samples were prepared by drop casting the suspended aggregates in solution onto silica substrates followed by Pt sputtering on the surface. Fluorescence-mode optical microscopic images were obtained on an inverted fluorescence microscope (Olympus ×71). Confocal laser scanning microscopy (CLSM) images were obtained on an Olympus FV1000 inverted confocal laser scanning microscope coupled with a continuous wave laser (405 nm, 2.5 W mm$^{-2}$). XRD measurements were conducted on a PANalytical X'Pert PRO instrument (40 kV, 200 mA). UV−vis absorption spectra were measured on a Hitachi U-3900 UV−vis spectrophotometer. The fluorescence quantum yields of **1** micelles were determined by the integrating sphere method performed on a Hamamatsu Absolute PL Quantum Yield spectrometer C11247.

**Preparation of Meat Samples.** Live bass were purchased at the market. Then, they were slaughtered, sliced, and brought back to the laboratory. Additionally, live shrimp were purchased, and the shrimp meat was prepared in the laboratory for testing. Chilled fresh chicken (breasts) and pork (tenderloins) were obtained via same-day delivery from a supplier. To monitor meat freshness, 5 g samples of the meat products (i.e., chicken, shrimp, pork, and fish) were placed in an open vial (20 mL) at room temperature (22 °C) for different amounts of time. Before testing, these meat samples were sealed for 1 min to accumulate the volatile components emitted. The accumulated volatiles in the sealed vials were then released for 5 s and sucked into a sensor array or into a proton-transfer reaction time-of-flight mass spectrometry (PTR-ToF-MS) instrument for further testing. Five grams of the refrigerated meat samples were prepared by cutting the meat products that were stored at 5 °C for different amounts of time. Before testing, the temperature of the refrigerated meat samples was first allowed to rise to 22 °C, and then they were sealed for 1 min to collect the emitted volatiles.

**Meat Samples for Real-World Application.** 100 g of chicken (breasts) and pork (tenderloins) were purchased at a farmers market where the meat products (e.g., pork and chicken) were kept on the shelf at room temperature throughout the day to sell. Before testing, 5 g of chicken and pork were cut off from the bulk meat and sealed in a vial (20 mL) at room temperature (22 °C) for 1 min to accumulate the emitted volatiles.

**Proton-Transfer Reaction Time-of-Flight Mass Spectrometry (PTR-ToF-MS) Measurements.** A PTR-ToF-MS 1000 (IONICON, Austria) instrument was used to determine the emitted VOCs and their absolute quantities released from the meat samples. The volatiles from the meat that accumulated in the sealed vials (20 mL) over 1 min were released for 5 s and sucked into a PTR-ToF-MS instrument through PEEK tubing for analysis. The PTR-ToF-MS spectra were recorded at a time resolution of 1 s with an inlet flow rate of 150 sccm. The $H_3O^+$ ionization mode was chosen with a drift voltage of 600 V, a drift temperature of 70 °C, and a drift pressure of 2.20 mbar, resulting in an E/N ratio of approximately 139 Td (1 Td = $10^{-17}$ cm$^2$/V).

**Fluorescence Sensing.** The optical chambers for fluorescence sensing were prepared by casting 10 $\mu$L of **1** micelles or **2** aggregate suspension in methanol inside a quartz tube approximately 0.3 cm away from the air inlet. The remaining methanol was removed from the quartz tube by a capillary. Then, the resulting aggregates inside the quartz tube were dried for 1 min by a blower. The optical chamber could be integrated into a custom-built device with an ultrasensitive silicon diode detector (see Figure S1) or with an Ocean Optics USB4000-fluorometer as a detector that produces spectra with lower sensitivities (a 385 nm LED lamp as the light source, 0.05 mW/cm$^2$).[16] For both types of devices, real-time fluorescence trajectories were recorded when 5 mL of the volatile analytes at certain concentrations was pumped into the optical chamber (air pump rate, 150 mL/min). A vial (20 mL) containing 2 mL of the analytes (e.g., organic sulfides and other VOCs) was sealed overnight to achieve saturated vapor concentrations. The diluted vapor concentrations of the analytes were obtained by injecting a small volume of the saturated vapor into a sealed flask (500 mL). Hydrogen sulfide gas at 1 ppm in nitrogen was directly purchased from Dalian Special Gases Co., Ltd.

**Theoretical Calculations.** The ground-state geometry of molecules was optimized by a Gaussian 09 package[26] using the B3LYP/6-311G** atomic basis set at the DFT level. The binding energies were calculated at the M062X/6-311G** level with a correction for the basis set superposition error (BSSE). The binding energies between the fluorophores (**1** and **2**) and dimethyl sulfide were calculated to be 13.26 and 7.72 kcal/mol, respectively.


https://doi.org/10.1021/acssensors.2c00079
ACS Sens. 2022, 7, 1395−1402

**Theoretical Limit of Detection (LOD).** Based on previous reports,[16,27] the LODs of **1** micelles and **2** aggregates can be calculated using the following equation:

$$\mathrm{LOD} = 3 \times \mathrm{RMS}_{\mathrm{noise}}/\mathrm{slope} \quad (1)$$

where $\mathrm{RMS}_{\mathrm{noise}}$ is the root-mean-square value of the noise, which can be calculated by using eq 2:

$$\mathrm{RMS}_{\mathrm{noise}} = \sqrt{\frac{\sum (I_i - I_f)^2}{N \times (I_0)^2}} \quad (2)$$

Here, the slope values were calculated to be 0.306% and 0.026% for **1** micelles and **2** aggregates, respectively. $I_i$ and $I_f$ are the experimental and fitted fluorescence intensity values, respectively. $I_0$ is the fluorescence intensity value when $t$ is equal to 0. $N$ represents the number of data points (500 data points were used in this work; see Figure S9 in Supporting Information). The $\mathrm{RMS}_{\mathrm{noise}}$ values were calculated to be 0.0024% for **1** micelles or **2** aggregates. Based on the resulting $\mathrm{RMS}_{\mathrm{noise}}$ and the slope of the calibration curve, the theoretical LODs of **1** micelles and **2** aggregates could be obtained.

## RESULTS AND DISCUSSION

**Design of Fluorophore 1.** Inspired by the D−A fluorophore **2**, which can sensitively sense sulfur mustard via sulfur−$\pi$ interactions,[13] fluorophore **1**, which has a benzoselenadiazole group, was designed for monitoring meat freshness. Fluorophore **1** was expected to exhibit enhanced sensitivity to organic sulfides, because the benzoselenadiazole group has relatively deep $\sigma$ holes[28,29] and thereby can form strong chalcogen bonds with organic sulfides. Despite its lower sensitivity, as evidenced in the following observations, fluorophore **2** can assist in the assessment of the extent of meat spoilage, i.e., slight or severe spoilage. Therefore, fluorophores **1** and **2** were collectively applied to construct a two-member sensor array for monitoring meat freshness and for discerning the different stages of meat spoilage (Figure S1).

**Morphological and Optical Properties of 1 Micelles.** SEM revealed that fluorophore **1** formed irregular micelles with diameters of approximately 100 nm and with lengths of hundreds of nanometers (Figure 1a and b). CLSM showed that **1** micelles self-assembled in solution rather than forming from solvent evaporation (Figure S2) and remained stable for one month. No X-ray diffraction peaks for **1** micelles were observed, indicating a lack of ordered packing in fluorophore **1** (Figure S3). When excited by 340−390 nm UV light, **1** micelles exhibited orange fluorescence with a fluorescence quantum yield (FQY) of approximately 27% (Figure 1c), which was much lower than that of **1** monomers in solution (e.g., 58% in chloroform). Optical spectroscopic characterizations showed a large Stokes shift for **1** monomer (approximately 100 nm), indicative of its charge-transfer (CT) characteristic. Compared with **1** monomer in cyclohexane, **1** micelles exhibited marked, red-shifted absorption and fluorescence spectra (Figure 1d). Given the CT nature and the twisted molecular structure of fluorophore **1** (Figure S4) that suppresses $\pi$-interactions, the redshift observed above and the decreased emission efficiency of **1** micelles are likely the result of the relatively strong dipole−dipole interactions between molecules of fluorophore **1**.

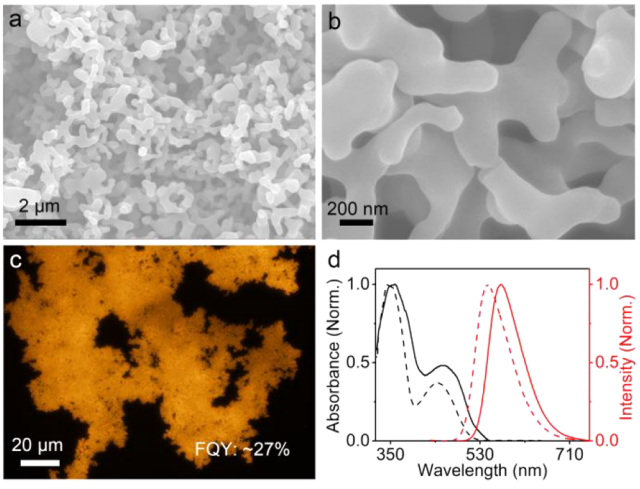


**Figure 1.** (a,b) SEM images of **1** micelles. (c) Fluorescence-mode optical microscopic image of **1** micelles. (d) Normalized absorption (black) and fluorescence spectra (red) of **1** micelles (solid) cast on a quartz slide and **1** monomer (dashed) in cyclohexane (2.5 $\mu$M).

**Sensing Performance of 1 Micelles and 2 Aggregates.** Prior to using **1** micelles and **2** aggregates to detect spoilage in meat samples, we first used PTR-ToF-MS to determine the VOCs, typically including organic sulfides and amines, and their absolute quantities released during meat spoilage. The volatiles emitted from 5 g of meat (e.g., chicken, shrimp, pork, and fish) in an open vial (20 mL) kept at room temperature for different durations (i.e., 10, 24, and 48 h) were accumulated for 1 min for PTR-ToF-MS measurements (details are outlined in the Experimental Section). Each meat sample was measured three times by PTR-ToF-MS, and similar results were obtained. Figures S5−8 and Tables S1−8 show the typical PTR-ToF-MS results for each kind of meat, where the various VOCs, particularly the organic sulfides or amines, and their absolute concentrations are listed in detail. When stored at room temperature for 10 h, all four kinds of meat emitted a small quantity of organic sulfides and amines, indicating that these meat products did not spoil substantially. At 24 h, a large increase in the amount of organic sulfides (hundreds of ppb) emitted was detected in the four meat samples, whereas much lower quantities of amines (tens of ppb) were detected. Shrimp was an exception, which emitted much greater quantities of dimethylamines (ca. 170 ppb), but the dimethylamine levels were still less than those of dimethyl sulfide (ca. 210 ppb). At 48 h, the quantity of organic sulfides released from the four meats was again much larger than that of the amines. Altogether, these observations indicate that the organic sulfides produced during meat spoilage are more volatile than the amines produced, thereby making them more suitable markers for the rapid assessment of meat freshness. Of note, many other VOCs were simultaneously released during meat spoilage, which may have masked or interfered with the responses of the sensor array to the organic sulfides. An evaluation of their effects on the responses of the sensor array to organic sulfides is shown below.

We next studied the sensitivity of **1** micelles to dimethyl sulfide, which is one of the main sulfur-containing compounds released as meats begin to spoil, as confirmed by PTR-ToF-MS and the literature.[5,30] To achieve high sensitivity, a device with a silicon diode detector (Figure S1) was applied to record the responses of the array when it was exposed to gas-phase dimethyl sulfide at different concentrations. As shown in Figure 2a, **1** micelles exhibited a remarkable degree of fluorescence quenching in response to dimethyl sulfide. When a device with an Ocean Optics USB4000 fluorometer for spectral recording but a low sensitivity was used, decreasing


https://doi.org/10.1021/acssensors.2c00079
ACS Sens. 2022, 7, 1395−1402

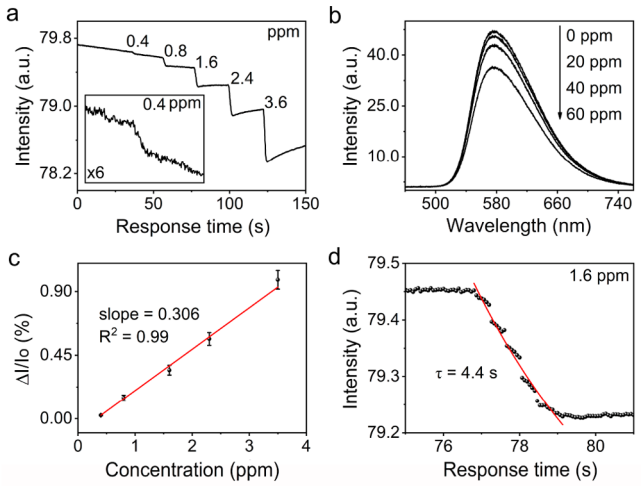


**Figure 2.** (a) Fluorescence quenching responses of **1** micelles (monitored in the range of 500−740 nm) to different concentrations of gaseous dimethyl sulfide. Note: these data were obtained by using a device with a silicon diode detector with high sensitivity. (b) Fluorescence spectra of **1** micelles upon exposure to different concentrations of gaseous dimethyl sulfide. Note: These data were obtained by using an Ocean Optics USB4000 fluorometer as the detector, which provides spectra but exhibits low sensitivity. (c) Experimental and fitted fluorescence quenching efficiency of **1** micelles upon exposure to different concentrations of gaseous dimethyl sulfide. The error bars represent the standard deviation of five measurements. (d) Response time of **1** micelles to gaseous dimethyl sulfide at 1.6 ppm, which was obtained by using first-order exponential curve fitting.

fluorescence spectral changes in **1** micelles were induced by gaseous dimethyl sulfide (Figure 2b), consistent with the changes in the fluorescence intensity, as shown in Figure 2a. Further analysis showed a linear relationship between the fluorescence quenching efficiency ($\Delta I/I_o$) of **1** micelles and the dimethyl sulfide concentrations (Figure 2c). On the basis of the resulting linear relationship and a signal-to-noise ratio of 3, the theoretical limit of detection (LOD) was calculated to be 23 ppb (details are outlined in the Experimental Section and Figure S9). We hypothesized that the low LOD was the result of the strong chalcogen bonding as well as the sulfur−$\pi$ interactions between **1** micelles and dimethyl sulfide. To support this hypothesis, the molecular distance and binding energy between fluorophore **1** and dimethyl sulfide were calculated at the M062X/6-311G** level. As shown in Figure S10, Se−S has a distance of 3.09 Å, indicative of the formation of a strong chalcogen bond with a binding energy of 13.26 kcal/mol. The low LOD of **1** micelles is significant because it allows for the detection of organic sulfides even at very low concentrations. Notably, the fluorescence quenching response of **1** micelles was fast, i.e., ∼4.4 s, which is favorable for practical applications (Figure 2d). Of note, the fluorescence intensity of **1** micelles decreased continuously with irradiation time. Given that **1** micelles were much more stable in argon than in air (Figure S11a), the decrease in fluorescence likely originated from an oxygen-induced photooxidation reaction. However, the zero-point shift had a negligible effect on the detection repeatability. As shown in Figure S11, steady fluorescence quenching responses were observed upon exposure of **1** micelles before and after 3 h of UV irradiation to 0.8 ppm gaseous dimethyl sulfide five times. In addition, **1** micelles exhibited sensitive responses to the dimethyl disulfide that was released due to meat spoilage (LOD, 7.7 ppm), but no response to hydrogen sulfides were observed (Figure S12).

To highlight the effect of chalcogen bonding, we tested and compared the sensing performance of fluorophore **2**, which had relatively weak chalcogen bonding with dimethyl sulfide. Using the same method, the theoretical LOD of **2** aggregates for dimethyl sulfide was calculated to be 280 ppb (Figure S13), which was 1 order of magnitude greater than that of **1** micelles. This also means that **2** aggregates could only detect organic sulfides at relatively high concentrations.

Given that water, amines, and other VOCs are simultaneously released during the course of meat spoilage, we tested the responses of **1** micelles and **2** aggregates to these volatiles and assessed their effects on the selectivity of **1** micelles and **2** aggregates to organic sulfides. As shown in Figures 3, S14, and S15, **1** micelles and **2** aggregates exhibited either a reversible enhancement or negligible responses to water and most VOCs at relatively high concentrations, whereas they gave irreversibly enhanced responses to amines at ppm concentrations (Figures 3b and S15). The reversibly enhanced responses can be explained by a swelling mechanism whereby most VOCs can cause swelling in **1** micelles and **2** aggregates temporarily and reduce intermolecular dipole−dipole interactions to enhance emission. A similar swelling mechanism has been demonstrated in polymer systems.[31] Given that the responses by most VOCs can be completely restored within 1−2 s, the irreversible quenching responses in response to organic sulfides can occur after the fast, reversible responses in response to other VOCs. Therefore, the fast, reversible responses induced by most VOCs will not mask the irreversible responses induced by organic sulfides. On the other hand, amines at ppm concentration have relatively strong interactions with fluorophores **1** and **2** (e.g., the dipole−dipole interaction) to induce irreversible responses that can mask the responses due to organic sulfides. Fortunately, the concentration of amines, as evidenced by the PTR-ToF-MS results, was far below the ppm levels; therefore, the amines induced negligible responses in **1** micelles and **2** aggregates. Figure 3e summarizes the responses of **1** micelles and **2** aggregates to dimethyl sulfides against various interferents, such as water, amines, and other VOCs, including common disinfectants used in meat factories (Figure S16), which demonstrates the high selectivity of **1** micelles and **2** aggregates to organic sulfides against various interferents.

Having confirmed the different sensitivities of **1** micelles and **2** aggregates to organic sulfides, we next explored whether **1** micelles could be used to monitor transitions from freshness to slight spoilage in meat, while **2** aggregates could assess the extent of meat spoilage. To this end, **1** micelles and **2** aggregates were fabricated into a two-member sensor array for monitoring meat spoilage, as shown in Figure S1. Here, on the basis of the combined responses of the two members, we defined three stages of meat spoilage, i.e., freshness (stage I), slight spoilage (stage II), and moderate or severe spoilage (Stage III). Specifically, the volatiles collected from the meats during stage I caused no quenching responses in both **1** micelles and **2** aggregates; the volatiles collected from the meats during stage II gave rise to a quenching response of **1** micelles but no response of **2** aggregates; the volatiles collected from the meats during stage III result in a quenching response of both **1** micelles and **2** aggregates. Figure 4 shows the distinct fluorescence responses to the time-dependent volatiles emitted from the four meats. Enhanced responses were observed but no quenching responses were observed upon exposure of both


https://doi.org/10.1021/acssensors.2c00079
ACS Sens. 2022, 7, 1395−1402

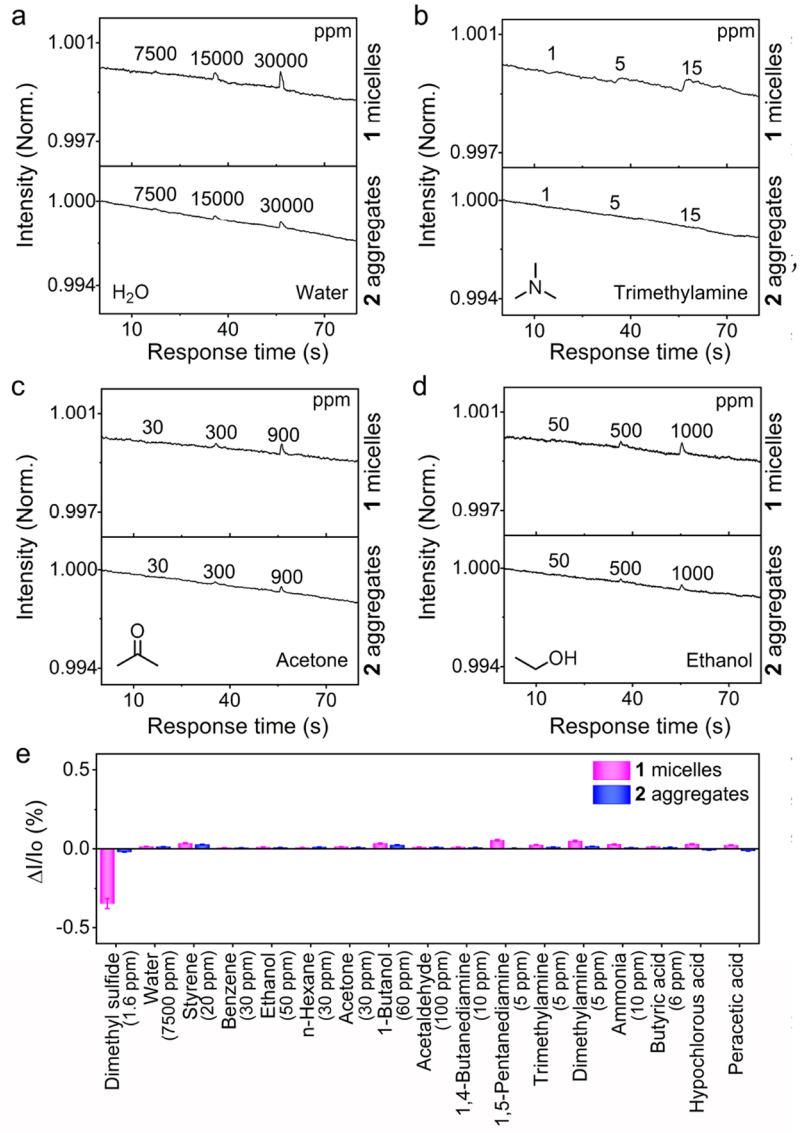


**Figure 3.** Fluorescence responses of **1** micelles and **2** aggregates to water (a), trimethylamine (b), acetone (c), and ethanol (d) at different concentrations. Note: these data were obtained by using a device with a silicon diode detector with high sensitivity. (e) Columnar comparison of the fluorescence responses of **1** micelles and **2** aggregates upon exposure to dimethyl sulfide and various potential interferents. $\Delta I/I_0$ represents the change in fluorescence intensity. The error bars represent the standard deviation of five measurements.

**1** micelles and **2** aggregates to the volatiles collected from the four meat products kept at room temperature for 18 h, a time period that was assigned to stage I. Here, the observed enhanced responses were restored within 1−2 s (Figure 4), consistent with the aforementioned responses caused by most VOCs (Figure 3) in the absence of organic sulfides. During this stage, very low concentrations of organic sulfides below the LOD of **1** micelles were released, which agrees with the PTR-ToF-MS results (at 10 h), indicative of the freshness of these meat products. Intriguingly, the exposure of **1** micelles to the volatiles from the meats kept at room temperature for prolonged period of time (e.g., 1 d) gave quenching responses following the initial enhanced responses.

Simultaneously, the exposure of **2** aggregates to the same volatiles yielded no quenching responses but did exhibit enhanced responses. These results indicate that at this stage (termed stage II), organic sulfides were emitted because of meat spoilage, but they were at such low concentrations that they could not be sensed by **2** aggregates, which have a relatively low sensitivity. Of note, the spoilage process could be largely delayed by storing the meat products at colder temperatures, e.g., at 5 °C. As shown in Figure S17, **1** micelles only began to exhibit fluorescence quenching responses when they were exposed to the volatiles collected from the bass samples stored at 5 °C for more than 132 h. This demonstrates the greatly delayed time point for the onset of stage II for refrigerated fish compared with that of fish kept at room temperature. For the refrigerated pork, chicken, and shrimp samples, the time points for the onset of stage II were further delayed to 144 h, as shown in Figure S17. Following the aforementioned standard curves and assuming the responses were caused by only dimethyl sulfide, the estimated (fitted) concentrations of the dimethyl sulfides released from the four meats at 24 h fell in the range of 400−600 ppb (Tables S9−12). Within some degree of error, the results at the corresponding time points agreed with those of the PTR-


https://doi.org/10.1021/acssensors.2c00079
ACS Sens. 2022, 7, 1395−1402

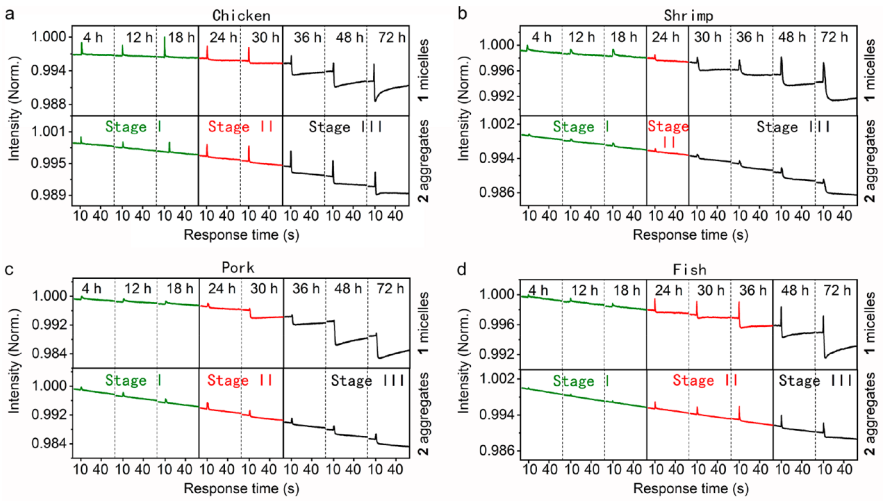


**Figure 4.** Fluorescence responses of **1** micelles and **2** aggregates to the volatiles collected over 1 min from 5 g of the meat products that were stored at room temperature for various durations: (a) chicken, (b) shrimp, (c) pork, and (d) fish.

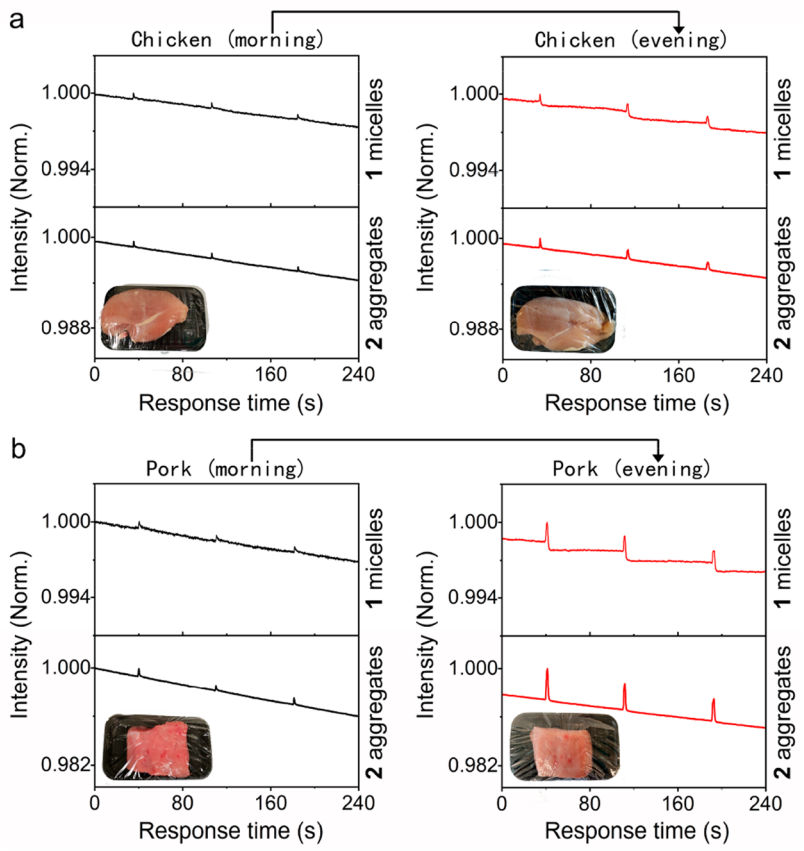


**Figure 5.** Fluorescence responses of **1** micelles and **2** aggregates to the volatiles collected from (a) the chicken sold in the morning and chicken left until the evening; (b) the pork sold in the morning and pork left until the evening.

ToF-MS results, supporting the reliability of our sensor array for the detection of organic sulfides. Herein, stage II could be considered the stage at which a slight degree of spoilage occurred. As the spoilage time progressed, **1** micelles began to exhibit substantial fluorescence quenching, and **2** aggregates exhibited distinct quenching responses when exposed to the volatiles from the meats. These observations indicate that increasing amounts of organic sulfides were released as a consequence of severe spoilage (termed Stage III). During this stage, typically at 48 h, the estimated concentrations for the dimethyl sulfide released from the four meats fell in the range of 900−3000 ppb (Table S9−12), consistent within error with the PTR-ToF-MS results, again corroborating the reliability of our sensor array.

Altogether, the preceding results highlight the capacity of the sensor array comprising **1** micelles and **2** aggregates to quickly assess the three stages of meat spoilage, including fresh, slightly



https://doi.org/10.1021/acssensors.2c00079
ACS Sens. 2022, 7, 1395−1402

spoiled, and moderately or severely spoiled, which is highly favorable in practical applications.

**Real-World Applications.** To further illustrate the practicability of the two-member sensor array, we utilized the developed sensor to test the freshness of meat products that were sold in at a farmers market where the meat products (e.g., pork and chicken) were kept on the shelf at room temperature throughout the day to sell. As shown in Figure 5, both **1** micelles and **2** aggregates exhibited no fluorescence quenching but did exhibit enhanced responses when exposed to the volatiles from the chicken and pork sold in the morning, indicating meat freshness, because these meats released negligible quantities of organic sulfides at this time point. In contrast, the exposure of **1** micelles and **2** aggregates to the volatiles emitted from some of the chicken and pork products that remained in the evening gave fluorescence quenching following an initially enhanced response and a reversibly enhanced response only, respectively, indicating that the meat products that remained in the evening were at a stage II of spoilage (i.e., slight spoilage). These results demonstrate that the two-member sensor array enables the fast assessment of meat freshness in the real world.

## CONCLUSIONS

In conclusion, we developed two D−A fluorophores **1** and **2** with differential sensitivities to organic sulfides and utilized them to fabricate a two-member sensor array for monitoring the stages of meat spoilage by the fluorescence detection of organic sulfides as a freshness indicator. We demonstrated that the first member of the array (i.e., **1** micelles) had a much higher sensitivity to organic sulfides than **2** aggregates, which enabled monitoring of the transition from fresh (Stage I) to slightly spoiled (Stage II) in meat products, while the second member could assist in assessing the extent of meat spoilage. Altogether, the two-member sensor array enabled the assessment of the stage of spoilage for a given meat product, which included fresh, slightly spoiled, and moderately or severely spoiled. Furthermore, this sensor array required a short duration of 1 min for the collection of volatiles from the meat products, which greatly facilitates its practical applications.

## ASSOCIATED CONTENT

### Supporting Information

The Supporting Information is available free of charge at https://pubs.acs.org/doi/10.1021/acssensors.2c00079.

Synthetic procedure, property and sensing characterizations, XRD, CLSM, theoretical calculations, PTR-ToF-MS, and other fluorescence responses (PDF)

## AUTHOR INFORMATION


### Corresponding Authors

**Chunxiao Lv** − *Key Laboratory of Photochemistry, CAS Research/Education Center for Excellence in Molecular Sciences, Institute of Chemistry, Chinese Academy of Sciences, Beijing 100190, China; University of Chinese Academy of Sciences, Beijing 100049, China*; Email: ykche@iccas.ac.cn

**Yanke Che** − *Key Laboratory of Photochemistry, CAS Research/Education Center for Excellence in Molecular Sciences, Institute of Chemistry, Chinese Academy of Sciences, Beijing 100190, China; University of Chinese Academy of Sciences, Beijing 100049, China*; orcid.org/0000-0002-9671-3704; Email: lyuchx@iccas.ac.cn

### Authors

**Xinting Yu** − *Key Laboratory of Photochemistry, CAS Research/Education Center for Excellence in Molecular Sciences, Institute of Chemistry, Chinese Academy of Sciences, Beijing 100190, China; University of Chinese Academy of Sciences, Beijing 100049, China*

**Yanjun Gong** − *Key Laboratory of Photochemistry, CAS Research/Education Center for Excellence in Molecular Sciences, Institute of Chemistry, Chinese Academy of Sciences, Beijing 100190, China; University of Chinese Academy of Sciences, Beijing 100049, China*

**Hongwei Ji** − *Key Laboratory of Photochemistry, CAS Research/Education Center for Excellence in Molecular Sciences, Institute of Chemistry, Chinese Academy of Sciences, Beijing 100190, China; University of Chinese Academy of Sciences, Beijing 100049, China*

**Chuanqin Cheng** − *Key Laboratory of Photochemistry, CAS Research/Education Center for Excellence in Molecular Sciences, Institute of Chemistry, Chinese Academy of Sciences, Beijing 100190, China; University of Chinese Academy of Sciences, Beijing 100049, China*

**Yifan Zhang** − *Key Laboratory of Photochemistry, CAS Research/Education Center for Excellence in Molecular Sciences, Institute of Chemistry, Chinese Academy of Sciences, Beijing 100190, China; University of Chinese Academy of Sciences, Beijing 100049, China*; orcid.org/0000-0003-1298-5436

**Ling Zang** − *Department of Material Science and Engineering, University of Utah, Salt Lake City, Utah 84112, United States*; orcid.org/0000-0002-4299-0992

**Jincai Zhao** − *Key Laboratory of Photochemistry, CAS Research/Education Center for Excellence in Molecular Sciences, Institute of Chemistry, Chinese Academy of Sciences, Beijing 100190, China; University of Chinese Academy of Sciences, Beijing 100049, China*; orcid.org/0000-0003-1449-4235

Complete contact information is available at: https://pubs.acs.org/10.1021/acssensors.2c00079


### Notes

The authors declare no competing financial interest.

## ACKNOWLEDGMENTS

This work was supported by the National Key Research and Development Program of China (No. 2019YFA0210401), the NSFC (Nos. 21925604), the Strategic Priority Research Program of the Chinese Academy of Sciences (Grant No. XDB36000000), and the China Postdoctoral Science Foundation (No. 2020M680681).

## REFERENCES

(1) Jia, R.; Tian, W.; Bai, H.; Zhang, J.; Wang, S.; Zhang, J. Amine-Responsive Cellulose-Based Ratiometric Fluorescent Materials for Real-Time and Visual Detection of Shrimp and Crab Freshness. *Nat. Commun.* **2019**, *10*, 795.

(2) Hu, Y.; Ma, X.; Zhang, Y.; Che, Y.; Zhao, J. Detection of Amines with Fluorescent Nanotubes: Applications in the Assessment of Meat Spoilage. *ACS Sens* **2016**, *1*, 22−25.

(3) Liu, S. F.; Petty, A. R.; Sazama, G. T.; Swager, T. M. Single-walled Carbon Nanotube/Metalloporphyrin Composites for the

Chemiresistive Detection of Amines and Meat Spoilage. *Angew. Chem., Int. Ed.* **2015**, *54*, 6554−6557.
(4) Kim, H.; Trinh, B. T.; Kim, K. H.; Moon, J.; Kang, H.; Jo, K.; Akter, R.; Jeong, J.; Lim, E. K.; Jung, J.; Choi, H. S.; Park, H. G.; Kwon, O. S.; Yoon, I.; Kang, T. Au@ZIF-8 SERS Paper for Food Spoilage Detection. *Biosens. Bioelectron.* **2021**, *179*, 113063.
(5) Li, Z.; Suslick, K. S. Portable Optoelectronic Nose for Monitoring Meat Freshness. *ACS Sens* **2016**, *1*, 1330−1335.
(6) Wang, B.; Wang, X.; Zeng, A.; Leng, J.; Zhao, W. Engineering a Mitochondria-Targeted Ratiometric Fluorescent Probe with a Large Stokes Shift for $H_2S$-Specific Assaying in Foodstuffs and Living Cells. *Sens. Actuators, B* **2021**, *343*, 130095.
(7) Pei, X.; Hu, J.; Song, H.; Zhang, L.; Lv, Y. Ratiometric Cataluminescence Sensor of Amine Vapors for Discriminating Meat Spoilage. *Anal. Chem.* **2021**, *93*, 6692−6697.
(8) Lai, F.; Yang, J.; Huang, R.; Wang, Z.; Tang, J.; Zhang, M.; Miao, R.; Fang, Y. Nondestructive Evaluation of Fish Freshness through Nanometer-Thick Fluorescence-Based Amine-Sensing Films. *ACS Appl. Nano Mater.* **2021**, *4*, 2575−2582.
(9) Alam, P.; Leung, N. L.; Su, H.; Qiu, Z.; Kwok, R. T.; Lam, J. W.; Tang, B. Z. A Highly Sensitive Bimodal Detection of Amine Vapours Based on Aggregation Induced Emission of 1, 2-Dihydroquinoxaline Derivatives. *Chem.—Eur. J.* **2017**, *23*, 14911−14917.
(10) Quan, Z.; He, H.; Zhou, H.; Liang, Y.; Wang, L.; Tian, S.; Zhu, H.; Wang, S. Designing an Intelligent Nanofiber Ratiometric Fluorescent Sensor Sensitive to Biogenic Amines for Detecting the Freshness of Shrimp and Pork. *Sens. Actuators, B* **2021**, *333*, 129535.
(11) Roy, R.; Sajeev, N. R.; Sharma, V.; Koner, A. L. Aggregation Induced Emission Switching Based Ultrasensitive Ratiometric Detection of Biogenic Diamines Using a Perylenediimide-Based Smart Fluoroprobe. *ACS Appl. Mater. Interfaces.* **2019**, *11*, 47207−47217.
(12) Qi, X. N.; Che, Y. X.; Qu, W. J.; Zhang, Y. M.; Yao, H.; Lin, Q.; Wei, T. B. Design and Fabricating Biogenic Amine-Responsive Platform Based on Self-Assembly Property of Phenazine Derivative for Visual Monitoring of Meat Spoilage. *Sens. Actuators, B* **2021**, *333*, 129430.
(13) Cui, L.; Gong, Y.; Cheng, C.; Guo, Y.; Xiong, W.; Ji, H.; Jiang, L.; Zhao, J.; Che, Y. Highly Photostable and Luminescent Donor-Acceptor Molecules for Ultrasensitive Detection of Sulfur Mustard. *Adv. Sci.* **2021**, *8*, 2002615.
(14) Qiu, C.; Gong, Y.; Guo, Y.; Zhang, C.; Wang, P.; Zhao, J.; Che, Y. Sensitive Fluorescence Detection of Phthalates by Suppressing the Intramolecular Motion of Nitrophenyl Groups in Porous Crystalline Ribbons. *Anal. Chem.* **2019**, *91*, 13355−13359.
(15) Gong, Y.; Guo, Y.; Qiu, C.; Zhang, Z.; Zhang, F.; Wei, Y.; Wang, S.; Che, Y.; Wei, J.; Yang, Z. Integrative Self-Assembly of Covalent Organic Frameworks and Fluorescent Molecules for Ultrasensitive Detection of a Nerve Agent Simulant. *Sci. China Mater.* **2021**, *64*, 1189−1196.
(16) Cui, L.; Gong, Y.; Yu, X.; Lv, C.; Du, X.; Zhao, J.; Che, Y. Development of a Fluorophore with Enhanced Unorthodox Chalcogen Bonding for Highly Sensitive Detection of Trimethyl Arsine Vapor. *ACS Sens* **2021**, *6*, 2851−2857.
(17) Liu, K.; Shang, C.; Wang, Z.; Qi, Y.; Miao, R.; Liu, K.; Liu, T.; Fang, Y. Non-Contact Identification and Differentiation of Illicit Drugs using Fluorescent Films. *Nat. Commun.* **2018**, *9*, 1695.
(18) Liu, H.; Saito, Y.; Riza, D. F. A.; Kondo, N.; Yang, X.; Han, D. Rapid Evaluation of Quality Deterioration and Freshness of Beef During Low Temperature Storage Using Three-Dimensional Fluorescence Spectroscopy. *Food Chem.* **2019**, *287*, 369−374.
(19) Wu, D.; Sedgwick, A. C.; Gunnlaugsson, T.; Akkaya, E. U.; Yoon, J.; James, T. D. Fluorescent Chemosensors: The Past, Present and Future. *Chem. Soc. Rev.* **2017**, *46*, 7105−7123.
(20) Lee, M. H.; Kim, J. S.; Sessler, J. L. Small Molecule-Based Ratiometric Fluorescence Probes for Cations, Anions, and Biomolecules. *Chem. Soc. Rev.* **2015**, *44*, 4185−4191.
(21) Wang, F.; Wang, L.; Chen, X.; Yoon, J. Recent Progress in the Development of Fluorometric and Colorimetric Chemosensors for Detection of Cyanide Ions. *Chem. Soc. Rev.* **2014**, *43*, 4312−4324.
(22) Thomas, S. W.; Joly, G. D.; Swager, T. M. Chemical Sensors Based on Amplifying Fluorescent Conjugated Polymers. *Chem. Rev.* **2007**, *107*, 1339−1386.
(23) Xu, X. Y.; Lian, X.; Hao, J. N.; Zhang, C.; Yan, B. A. Double-Stimuli-Responsive Fluorescent Center for Monitoring of Food Spoilage Based on Dye Covalently Modified EuMOFs: From Sensory Hydrogels to Logic Devices. *Adv. Mater.* **2017**, *29*, 1702298.
(24) Koskela, J.; Sarfraz, J.; Ihalainen, P.; Määttänen, A.; Pulkkinen, P.; Tenhu, H.; Nieminen, T.; Kilpelä, A.; Peltonen, J. Monitoring the Quality of Raw Poultry by Detecting Hydrogen Sulfide with Printed Sensors. *Sens. Actuators, B* **2015**, *218*, 89−96.
(25) Yuan, Z.; Bariya, M.; Fahad, H. M.; Wu, J.; Han, R.; Gupta, N.; Javey, A. Trace-Level, Multi-Gas Detection for Food Quality Assessment Based on Decorated Silicon Transistor Arrays. *Adv. Mater.* **2020**, *32*, 1908385.
(26) Frisch, M. J.; Trucks, G. W.; Schlegel, H. B.; Scuseria, G. E.; Robb, M. A.; Cheeseman, J. R.; Scalmani, G.; Barone, V.; Mennucci, B.; Petersson, G. A.; Nakatsuji, H.; Caricato, M.; Li, X.; Hratchian, H. P.; Izmaylov, A. F.; Bloino, J.; Zheng, G.; Sonnenberg, J. L.; Hada, M.; Ehara, M.; Toyota, K.; Fukuda, R.; Hasegawa, J.; Ishida, M.; Nakajima, T.; Honda, Y.; Kitao, O.; Nakai, H.; Vreven, T.; Montgomery, J. A.; Peralta, J. E.; Ogliaro, F.; Bearpark, M.; Heyd, J. J.; Brothers, E.; Kudin, K. N.; Staroverov, V. N.; Keith, T.; Kobayashi, R.; Normand, J.; Raghavachari, K.; Rendell, A.; Burant, J. C.; Iyengar, S. S.; Tomasi, J.; Cossi, M.; Rega, N.; Millam, J. M.; Klene, M.; Knox, J. E.; Cross, J. B.; Bakken, V.; Adamo, C.; Jaramillo, J.; Gomperts, R.; Stratmann, R. E.; Yazyev, O.; Austin, A. J.; Cammi, R.; Pomelli, C.; Ochterski, J. W.; Martin, R. L.; Morokuma, K.; Zakrzewski, V. G.; Voth, G. A.; Salvador, P.; Dannenberg, J. J.; Dapprich, S.; Daniels, A. D.; Farkas, O.; Foresman, J. B.; Ortiz, J. V.; Cioslowski, J.; Fox, D. J. *Gaussian 09*, Revision B.01; Gaussian, Inc.: Wallingford, CT, 2013.
(27) Zhao, S.; Shen, Y.; Maboudian, R.; Carraro, C.; Han, C.; Liu, W.; Wei, D. Facile Synthesis of ZnO-$SnO_2$ Hetero-structured Nanowires for High-performance $NO_2$ Sensing Application. *Sens. Actuators, B* **2021**, *333*, 129613.
(28) Lee, L. M.; Tsemperouli, M.; Poblador-Bahamonde, A. I.; Benz, S.; Sakai, N.; Sugihara, K.; Matile, S. Anion Transport with Pnictogen Bonds in Direct Comparison with Chalcogen and Halogen Bonds. *J. Am. Chem. Soc.* **2019**, *141*, 810−814.
(29) Benz, S.; Poblador-Bahamonde, A. I.; Low-Ders, N.; Matile, S. Catalysis with Pnictogen, Chalcogen, and Halogen Bonds. *Angew. Chem., Int. Ed.* **2018**, *57*, 5408−5412.
(30) Chow, C. F.; Ho, P. Y.; Sun, D.; Lu, Y. J.; Wong, W. L.; Tang, Q.; Gong, C. B. Development of Sensitive and Selective food Sensors Using New Re(I)-Pt(II) Bimetallic Complexes to Detect Volatile Biogenic Sulfides Formed by Meat Spoilage. *Food Chem.* **2017**, *216*, 382−389.
(31) Cox, J. R.; Muller, P.; Swager, T. M. Interrupted energy transfer: highly selective detection of cyclic ketones in the vapor phase. *J. Am. Chem. Soc.* **2011**, *133*, 12910−12913.


https://doi.org/10.1021/acssensors.2c00079
*ACS Sens.* 2022, 7, 1395−1402